MODELING AND ANALYSIS OF ROTOGRAVURE PRINTING PRESSES

By

A. Seshadri[1], P. R. Pagilla[1], and J. E. Lynch[2]
[1]Oklahoma State University
[2]Armstrong World Industries
USA

ABSTRACT

Print registration is the method of overlapping successive printed patterns to form a complex multicolor pattern. Registration error is the misalignment in the overlapped patterns. This paper deals with modeling machine direction registration error in a rotogravure printing press with multiple print units coupled by mechanical shafts. The model is developed by considering various dynamic elements in a print unit such as the print cylinder, doctor blade assembly, print unit compensator roller, cooling rollers, print unit motor, the effect of friction in various locations, etc. Experimental data from typical production runs on a print line is used to corroborate the model developed. Based on the developed model, mechanical design and control design recommendations to reduce registration error in print units are provided.

INTRODUCTION

The print line considered in this work consists of a print section with eight rotogravure print units, an unwind accumulator and a rewind accumulator for continuous processing of the composite web; a schematic of the print line is shown in Figure 1. Web tension and web transport velocity are regulated by pull roll 3 prior to the web entering the print section, and by pull roll 4 at the exit side of the print section. All eight print units in the print section are driven by a single print section drive motor. A common shaft connects the print section motor to the various print units through a mechanical transmission system. Each print unit consists of a print cylinder, an impression roller, back-up roller, cooling roller, registration error compensator, and several idle rollers that facilitate web transport from one print unit to the other. A schematic of a print unit is shown in Figure 2.

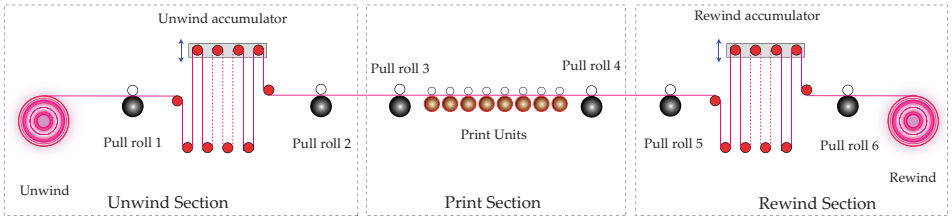

Figure 1: Print Line Schematic

The gravure print cylinder is engraved to form wells to create print patters on the cylinder surface. As the print cylinder rotates within the ink bath, ink is collected onto the wells or cells in the surface of gravure print cylinder. Excess ink from the surface of the print cylinder is scrapped by the doctor blade so that only the region of the gravure cylinder with the pattern collects the ink and the rest of the region is devoid of ink. As the web passes between the nipped impression roller and the print cylinder, the ink is transferred from the print cylinder to the web. The printed web with wet ink is transported over idle rollers in the drying section and cooled using a cooling roller downstream. The compensator roller, whose linear motion is controlled using a motor, is used to change the span length between successive print cylinders.

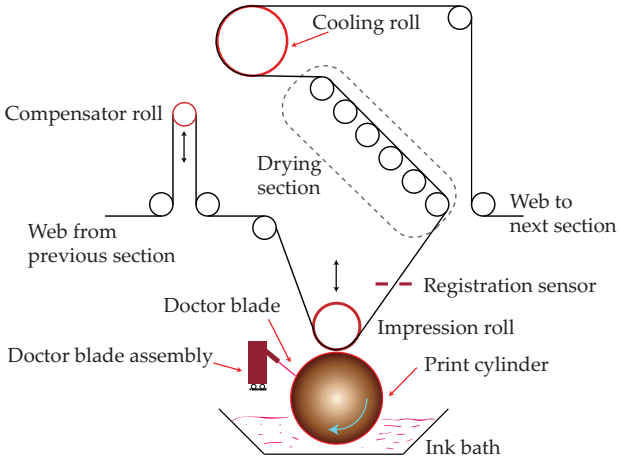

Figure 2: Individual Print Unit Schematic (individual elements are not to scale)

A complex print pattern with several colors may be created by successively overlapping individual patterns onto the web material as it passes through successive print units. When patterns are overlapped it is critical to align them to a create quality print output. Registration is the process of aligning successive print patterns on the web material.

Figure 3 shows a schematic of two successive print units. The first pattern is printed onto the web as it passes through the upstream print cylinder. Along with the pattern, a registration flag is also printed on the web near its edge. The next

pattern is printed on the web as it enters the downstream print cylinder. In order to ensure proper alignment of successive print patterns, the length of the web between the two print cylinders has to be an integer multiple of the circumference of upstream print cylinder (when both print cylinders are angularly aligned). The length of the web material between the print cylinders will be equal to the web path length if no sagging exists; this can be accomplished by maintaining appropriate tension in the web. Even though the web path length does not change, elongation of web results in misregistration; hence active registration control is needed to maintain print quality.

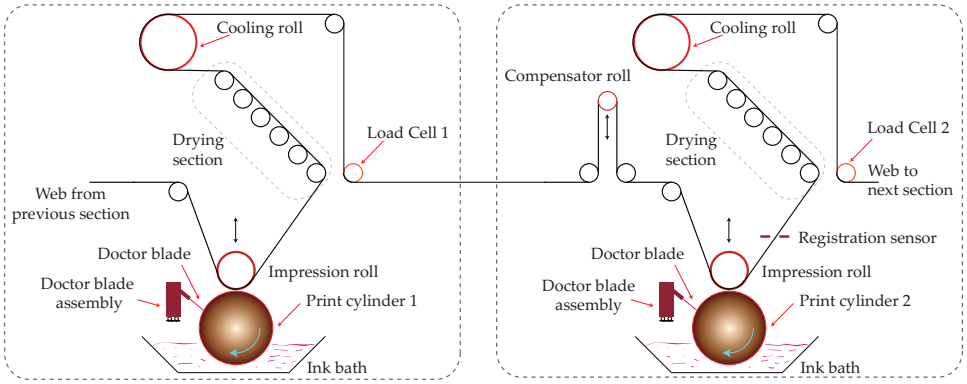

Figure 3: Schematic of Two Successive Print Units

The web path length is adjusted by using a compensator roller to correct for the registration error. As the second print pattern is printed onto the web, a registration flag is also printed along the edge of the web. A registration error sensor measures the distance between two successive registration flags. Based on the registration error, the compensator roller is moved to vary the web path length to compensate for the registration error and ensure proper registration.

Several web handling issues may contribute to occurrence of registration error. Issues such as web elongation, tension variations, print cylinder velocity variations, improper compensator motion, machine induced disturbances, and non-ideal transmissions. In this paper a first principles approach is followed to obtain a mathematical model for the registration error.

NOMENCLATURE

$\dot{(\,)}$	Derivative with respect to time
δ_{v_q}	Relative surface velocity between impression roller and q^{th} print cylinder
ϵ_1, ϵ_2	Web strain in spans upstream and downstream of print cylinder 1
$\overline{\epsilon}_{21}$	Strain difference between the downstream and upstream spans of a print cylinder $(\epsilon_2 - \epsilon_1)$
γ_{1_q}	Doctor blade contact angle at q^{th} print cylinder
μ_{pr_q}	Coefficient of friction between doctor blade and q^{th} print cylinder
μ_{sw_q}	Static friction coefficient between web and q^{th} print cylinder

μ_{dw_q}	Dynamic friction coefficient between web and q^{th} print cylinder
θ_1, ω_1, r_1	Angular position, velocity and radius of print cylinder 1
θ_2, ω_2, r_2	Angular position, velocity and radius of print cylinder 2
θ_m, ω_m	Angular position and velocity of print section motor
θ_q, ω_q	Angular position and velocity of common shaft at q^{th} position
$\theta_{pr_q}, \omega_{pr_q}$	Angular position and velocity of q^{th} print cylinder
$\theta_{dr_q}, \omega_{dr_q}$	Angular position and velocity of q^{th} doctor blade crank arm
ω_{Im_q}	Angular velocity of q^{th} impression roll
τ_1	Time constant for the web to travel from upstream print cylinder to downstream print cylinder
τ_2	Time constant for the web to travel from compensator roller to downstream print cylinder
A	Cross sectional area of the web
b_{dr_q}, J_{dr_q}	Viscous friction and moment of inertia of q^{th} doctor blade crank arm
b_{Im_q}, J_{Im_q}	Viscous friction and moment of inertia of q^{th} impression roll
b_m, J_m	Viscous friction and moment of inertia of print section motor
b_{pr_q}, J_{pr_q}	Viscous friction and moment of inertia of q^{th} print cylinder
b_q, J_q	Viscous friction and moment of inertia of common shaft at q^{th} position
e_r	Registration error
E	Modulus of elasticity of web
F	Friction force
F_{pr_q}	Friction force opposing print cylinder motion at q^{th} print cylinder
F_{dr_q}	Friction force opposing doctor blade motion at q^{th} print cylinder
F_{c_q}	Coulomb friction coefficient at q^{th} print cylinder
F_{v_q}	Viscous friction coefficient at q^{th} print cylinder
F_{D_q}	Load on the doctor blade at q^{th} print cylinder
F_{t_q}	Force due to tension differential at q^{th} impression roll
F_{f_q}	Force due to friction contact at q^{th} impression roll
F_{N_q}	Net normal force at q^{th} impression roll
F_{ni_q}	Nipping force at q^{th} impression roll
F_{nw_q}	Reaction force due to tension differential at q^{th} impression roll
K, K_{gr}	Transmission shaft and print unit gear box stiffness
L	Lagrangian
l	Nominal span length in a print unit (an integer multiple of upstream print cylinder circumference)
Δl	Change in span length from the nominal span length
M_{dr_q}	Mass of the doctor blade assembly at q^{th} print cylinder
n_{dr_q}	Transmission ratio between print section motor and doctor blade crank arm at q^{th} print cylinder
n_{dr_q}	Transmission ratio between print section motor and q^{th} print cylinder
r_{pr_q}, r_{Im_q}	Radius of q^{th} print cylinder and q^{th} impression roll
T	Total kinetic energy
T_1, T_2	Web tension in spans upstream and downstream of print cylinder 1
T_{i_q}, T_{i+1_q}	Web tension in spans upstream and downstream of q^{th} print cylinder
V	Total potential energy
v_{s_q}	Surface velocity of q^{th} print cylinder

v_{r_q}	Relative surface velocity between q^{th} print cylinder and q^{th} impression roll
V_1, V_2	Web velocity at print cylinder 1 and print cylinder 2
x_{dr_q}	Linear position of the doctor blade at q^{th} print cylinder
Subscripts	
q	print unit number; $q = l_1, \ldots, l_4, r_1, \ldots, r_4$

GOVERNING EQUATIONS FOR REGISTRATION ERROR

The governing equation for the registration error is derived in this section. Consider the print unit[1] shown in Figure 3. In the ideal case, when the web velocity at the two print cylinders is the same with no tension variation in the span between the print cylinders, the registration error would be zero if the web path length between the two print cylinders is an integer multiple of the upstream print cylinder circumference. But there are no ideal machine components and it is seldom possible to maintain ideal operating conditions. The occurrence of the registration error is mainly due to three main process conditions: tension variations, compensator roller linear velocity, and print cylinder velocity variations. It is assumed that each of these effects are independent and can be combined to obtain the registration error model. The following assumptions are considered:

- There is no slip between the web and the roller surface.
- The web strain is uniform along the length of the span.

The registration error due to the three main process conditions listed above is given by

$$e_r(t) = l - \int_{t-\tau_1}^{t} \frac{r_1\omega_1(\tau)}{1+\overline{\epsilon}_{21}(\tau)}d\tau - \left[r_2\theta_2(t) - \frac{r_1\theta_1(t-\tau_1)}{1+\overline{\epsilon}_{21}(t)}\right] + \int_{t-\tau_1}^{t-\tau_2} \dot{\Delta}l(\tau)d\tau. \quad \{1\}$$

The first integral in equation {1} is the length of the elongated web that passes through the upstream print cylinder during the time period τ_1. The second error term relates to the relative velocity variation between the two consecutive print cylinders on the registration error. The last term corresponds to the additional distance the web needs to travel due to the linear motion of the compensator roller.

As the web strains within the span between the two print cylinders the length of the printed image elongates. With a positive strain change, the net distance a portion of the printed image needs to travel reduces while with a negative strain the distance increases. Additionally, if the overall strain change as the web travels from the upstream print cylinder to the downstream print cylinder is zero, irrespective of the strain fluctuations in between, registration error is not affected by the strain fluctuations during the period τ_1. Hence the distance traveled by the printed web is compensated for the strain changes by the denominator term in the first integral. Unlike the model presented in [1], the strain variation above the nominal strain is not used, rather the relative strain between the upstream span and the downstream

[1]The print unit span is the span between the two print cylinders. The print unit number and span number corresponds to the upstream print cylinder number.

span of the print cylinder is used. This is because as long as the upstream and downstream span strains are the same (ϵ_1 and ϵ_2, respectively), the printed image is not elongated further after printing and hence will not affect the registration error; even if both ϵ_1 and ϵ_2 are not at their nominal values.

If the angular position and angular velocity of the two print cylinders are the same then a registration mark on the web from the upstream print cylinder at time $t-\tau_1$ would overlap exactly with a registration mark on downstream print cylinder at time t provided that the effect of strain variations and span length variations are neglected, that is, when $\theta_1(t-\tau_1) = \theta_2(t)$. But if the print cylinder velocities are not the same, then the registration error would be a function of the angular position difference between the two print cylinders. The error term in equation {1} represents the effect of print cylinder velocity variations on registration error. Note that the angular position error $\theta_1(t-\tau_1)$ at the upstream print cylinder at time $t-\tau_1$ is compensated for the strain variations as it reaches the downstream print cylinder with the denominator term $1+\overline{\epsilon}_{21}(t)$.

The compensator motion indirectly affects the registration error due to the strain variations; but the compensator motion also results in span length changes. As the compensator moves, the span length that the web needs to travel before reaching the next print cylinder increases or decreases. The distance traveled by the printed portion of web due to the motion of the compensator can be obtained from the net span length change during that period when the printed web travels from the upstream print cylinder to the downstream print cylinder. Note that the distance traveled by the web once it is past the compensator will always be the same. Hence when a printed portion of the web moves past the compensator roller, the compensator motion from that point forward in time would not change the span length L for that portion of the web. Hence the last integral in equation {1} compensates for the additional span length that the printed web needs to travel.

The registration error dynamics can be obtained from equation {1} by taking the time derivative and is given by

$$\begin{aligned}\dot{e}_r(t) = \; & r_2\omega_2(t) - r_1\left[\frac{1}{1+\overline{\epsilon}_{21}(t)}\left[\omega_1(t)-\omega_1(t-\tau_1)\right] - \frac{\omega_1(t-\tau_1)}{1+\overline{\epsilon}_{21}(t-\tau_1)}\right] \\ & - \frac{r_1\theta_1(t-\tau_1)\dot{\overline{\epsilon}}_{21}(t)}{\left[1+\overline{\epsilon}_{21}(t)\right]^2} + \left(\dot{\Delta}l(t-\tau_2) - \dot{\Delta}l(t-\tau_1)\right)\end{aligned} \quad . \qquad \{2\}$$

The model shown in equation {2} clearly shows the importance of tension regulation in both the upstream and downstream spans of the print cylinders. Note that the print cylinder velocities cannot be controlled independently, since they are driven by a single print section motor through compliant transmission elements. Additionally, there is no active control of web strain within the print unit span. The compensator roller is the only active element that can control the registration error in the print unit; but the motion of the compensator roller causes additional strain variations in that span. The following section will present a model for web strain in the print unit span considering the compensator motion, and a subsequent section will present the governing equations for the angular velocity of a print cylinder in a rotogravure printing press with multiple print units.

STRAIN DYNAMICS DUE TO COMPENSATOR MOTION

Figure 4 shows a schematic of a print unit with the compensator roller. The compensator roller is an active registration control device. The compensator roller is positioned linearly, using parallel ball screw mechanisms, to adjust the length of the span between the two print cylinders. If the angular velocity of the two print cylinders are maintained to be the same, then the web strain in the span can be maintained. But even when the two print cylinders rotate at the same speed, strain transport from the upstream spans and the motion of the compensator roller will affect the web strain in the considered print section span. A model that captures the effect of the compensator roller motion on web tension in that span is presented here.

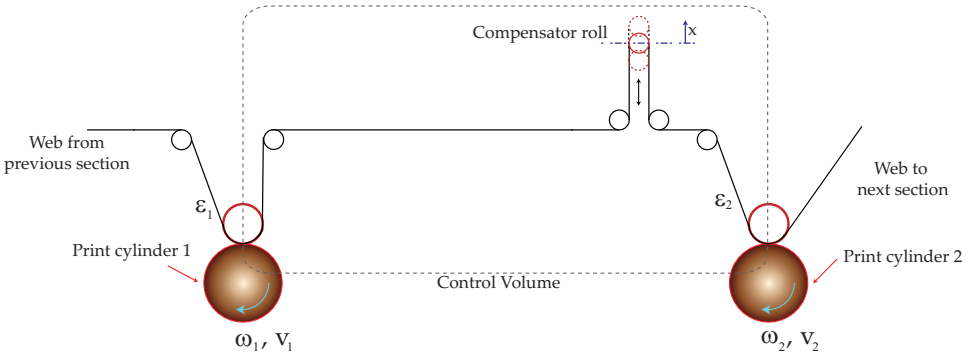

Figure 4: A simple schematic showing the web between two consecutive print cylinders; the effect of idle rollers is ignored.

Following the assumptions and procedure outlined in [2], and without the small strain assumption, the strain dynamics due compensator motion and print cylinder velocities can be obtained as

$$\dot{\epsilon}_2(t) = \frac{1+\epsilon_2(t)}{l+\Delta l(t)}\left[V_2(t) + \dot{\Delta} l(t) - V_1(t)\frac{1+\epsilon_2(t)}{1+\epsilon_1(t)}\right]; \qquad \{3\}$$

and the corresponding web tension dynamics, by assuming the web to be perfectly elastic, can be obtained as

$$\dot{T}_2(t) = \frac{EA+T_2(t)}{l+\Delta l(t)}\left[\left(V_2(t) + \dot{\Delta} l(t)\right) - V_1(t)\frac{EA+T_2(t)}{EA+T_1(t)}\right]. \qquad \{4\}$$

From the web strain dynamics with the compensator roller, it is evident that the compensator velocity and position affect the web strain in the print unit span. In order to maintain the same web strain, independent control of web velocity at the upstream and downstream print cylinders is necessary; and since the print cylinders cannot be controlled independently, movement of the compensator roller to minimize registration error would result in web strain variations in the span and consequently additional registration error. It has to be noted that the registration error dynamics given in the previous section is a retarded delay differential equation while the strain dynamics is an ordinary differential equation. The motion of the

compensator results in instantaneous strain changes while the registration error is an integral function over a period of time. Hence it may be possible that, with an appropriate control algorithm both strain changes and registration error may be reduced even without the independent control of individual print cylinders.

Even though independent control of print cylinder velocities is not possible in this case, understanding the print cylinder dynamics will be beneficial for designing a suitable control strategy for the compensator. The following section presents a dynamic model for print cylinder velocities and discusses causes for web velocity variations.

PRINT SECTION VELOCITY DYNAMICS

As described earlier, a single print section motor drives all the print cylinders. The print section motor transmits the power through a common shaft that drives individual gear boxes for each print unit. A device called the doctor blade is used to wipe excess ink off the print cylinder in order to obtain a quality print output. The doctor blade is mounted on a blade holder which pivots on an assembly frame. Figures 5 and 6 show a schematic of the doctor blade assembly. Pneumatic

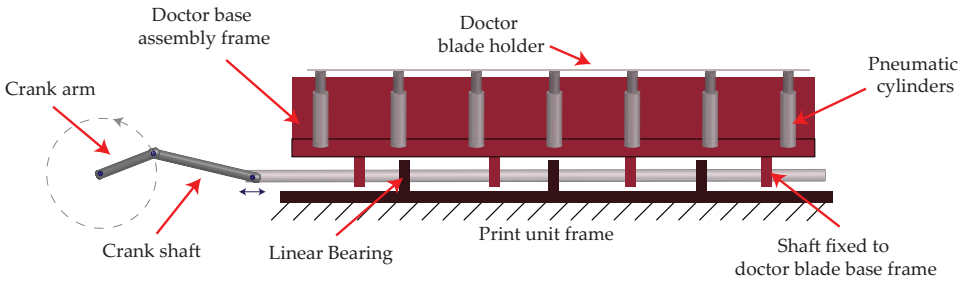

Figure 5: Doctor Blade Assembly

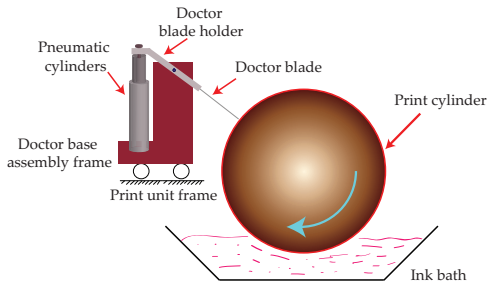

Figure 6: A side view of the doctor blade assembly and the print cylinder.

cylinders, housed on the doctor blade assembly frame, are used to apply pressure on the doctor blade holder such that adequate pressure is applied at the contact between the doctor blade and the print cylinder surface to wipe off excess ink.

In order to produce even wear on the doctor blade, the doctor blade is made to slide back and forth on the print cylinder as it wipes the ink off. To facilitate the

rocking motion the entire doctor blade assembly is moved back and forth. A linear bearing facilitates the sliding motion of the doctor blade assembly and a crank mechanism as shown in Figure 5 provides the power for the motion. Whenever the print cylinder is engaged by the clutch mechanism, the doctor blade assembly oscillates; but the doctor blade makes contact with the print cylinder only when the pneumatic cylinders are engaged. The frequency of oscillation of the doctor blade assembly is based on the gearing ratio and is usually fixed; the stroke length may be varied based on the crank arm radius. Since the same gear box drives the print cylinder and the doctor blade assembly, the motion of the doctor blade assembly will affect the print cylinder velocity dynamics. The print cylinder velocity dynamics is affected by the compliance in the transmission, the doctor blade assembly dynamics, and web tension in adjacent spans.

Print Cylinder Velocity Dynamics

A dynamic model of the print section can be obtained by appropriately combining the rotary motion of the print cylinders and the linear motion of the doctor blade assemblies in terms of the rotary motion of the print section motor using the Euler-Lagrange equations [3]. By considering compliant transmission elements, the dynamics of the individual print cylinders and doctor blade assemblies can be derived. The common shaft and the print unit gear box transmission elements are considered to be compliant but the crank arm and the crank shaft of the doctor blade assembly are assumed to be rigid.

The equations of motion are constructed using Euler-Lagrange equations by considering the total potential and kinetic energy in the print section. The total kinetic energy is given by

$$\begin{aligned} T = &\underbrace{\frac{1}{2}J_m\dot{\theta}_m^2}_{T_m} + \sum_{i=1}^{4}\underbrace{\frac{1}{2}J_{li}\dot{\theta}_{li}^2}_{T_{li}} + \sum_{i=1}^{4}\underbrace{\frac{1}{2}J_{ri}\dot{\theta}_{ri}^2}_{T_{ri}} + \sum_{i=1}^{4}\underbrace{\frac{1}{2}J_{pr_{li}}\dot{\theta}_{pr_{li}}^2}_{T_{pr_{li}}} + \sum_{i=1}^{4}\underbrace{\frac{1}{2}J_{pr_{ri}}\dot{\theta}_{pr_{ri}}^2}_{T_{pr_{ri}}} \\ &+ \sum_{i=1}^{4}\underbrace{\frac{1}{2}M_{dr_{li}}\dot{x}_{dr_{li}}^2}_{T_{dr_{li}}} + \sum_{i=1}^{4}\underbrace{\frac{1}{2}M_{dr_{r_i}}\dot{x}_{dr_{r_i}}^2}_{T_{dr_{ri}}} + \sum_{i=1}^{4}\underbrace{\frac{1}{2}J_{dr_{li}}\dot{\theta}_{dr_{li}}^2}_{T_{d_{li}}} + \sum_{i=1}^{4}\underbrace{\frac{1}{2}J_{dr_{r_i}}\dot{\theta}_{dr_{r_i}}^2}_{T_{d_{ri}}}. \end{aligned} \quad \{5\}$$

The total potential energy is given by

$$\begin{aligned} V = &\frac{1}{2}K(\theta_m - \theta_{l1})^2 + \frac{1}{2}K(\theta_m - \theta_{r1})^2 \\ &+ \frac{1}{2}K(\theta_{l1} - \theta_{l2})^2 + \frac{1}{2}K(\theta_{l2} - \theta_{l3})^2 + \frac{1}{2}K(\theta_{l3} - \theta_{l4})^2 \\ &+ \frac{1}{2}K(\theta_{r1} - \theta_{r2})^2 + \frac{1}{2}K(\theta_{r2} - \theta_{r3})^2 + \frac{1}{2}K(\theta_{r3} - \theta_{r4})^2 \\ &+ \frac{1}{2}K_{gr}\sum_{i=1}^{4}\left(\frac{\theta_{li}}{n_{pr_{li}}} - \theta_{pr_{li}}\right)^2 + \frac{1}{2}K_{gr}\sum_{i=1}^{4}\left(\frac{\theta_{ri}}{n_{pr_{ri}}} - \theta_{pr_{ri}}\right)^2 \\ &+ \frac{1}{2}K_{gr}\sum_{i=1}^{4}\left(\frac{\theta_{li}}{n_{dr_{li}}} - \theta_{dr_{li}}\right)^2 + \frac{1}{2}K_{gr}\sum_{i=1}^{4}\left(\frac{\theta_{ri}}{n_{dr_{ri}}} - \theta_{dr_{ri}}\right)^2. \end{aligned} \quad \{6\}$$

Note that the velocity of the doctor blade assembly may be obtained from the doctor

blade crank arm angular velocity by the following transformation (assuming crank arm and crank shaft to be rigid):

$$\dot{x}_q = -\left[r_q \sin\theta_q + \frac{r_q^2 \sin\theta_q \cos\theta_q}{\sqrt{l_q^2 - r_q^2 \sin^2\theta_q}} \right] \dot{\theta}_q, \quad q = dr_{li}, dr_{ri}, \quad i = 1, \ldots, 4 \qquad \{7\}$$

The Lagrangian L is given by

$$L = T - V \qquad \{8\}$$

and the equations of motion for the overall system using the generalized coordinate system may be obtained by using the following Euler-Lagrange equations:

$$\frac{d}{dt}\left(\frac{\partial L}{\partial \dot{q}_j}\right) - \frac{\partial L}{\partial q_j} = Q_j \qquad \{9\}$$

where q_j is the generalized coordinate and Q_j is the sum of the generalized forces acting on the system.

For the print section motor, the equation of motion can be obtained as

$$J_m \ddot{\theta}_m + K(\theta_m - \theta_{r1}) + K(\theta_m - \theta_{l1}) = \tau_m - b_m \dot{\theta}_m \qquad \{10\}$$

For the sake of brevity the common shaft dynamics is not shown but can be obtained in a similar fashion using the Euler-Lagrange equation. To derive the equations of motion for print cylinders, viscous bearing friction as well as the frictional effect of the doctor blade contact with the print cylinder surface are taken into consideration. In order to simplify the model, it is assumed that the friction force due to the axial motion of doctor blade does not affect the dynamics of the print cylinder; friction tangential to the surface of the roller at the doctor blade contact is considered. With that assumption, the dynamics for the print cylinders can be obtained as

$$J_{pr_q} \ddot{\theta}_{pr_q} + b_{pr_q} \dot{\theta}_{pr_q} = K_{gr}\left(\frac{\theta_q}{n_{pr_q}} - \theta_{pr_q}\right) - r_{pr_q} F_{pr_q} \qquad \{11a\}$$

where b_q is the viscous friction coefficient at the print cylinder bearing and F_{pr_q} is the tangential friction force due to the doctor blade contact.

The doctor blade assembly dynamics can be obtained from the Euler-Lagrange equations, which can be described in terms of the crank arm as

$$\begin{aligned} \underbrace{\left(M_{dr_q} f_q(\theta_{dr_q}) + J_{dr_q}\right)}_{J_{eq_{dr_q}}} \ddot{\theta}_{dr_q} =& K_{gr}\left(\frac{\theta_q}{n_{dr_q}} - \theta_{dr_q}\right) - \underbrace{\frac{1}{2} M_{dr_q} \frac{\partial f_q(\theta_{dr_q})}{\partial \theta_{dr_q}} \dot{\theta}_{dr_q}^2}_{W_{dr_q}} \\ & - F_{dr_q} g_q(\theta_{dr_q}) + b_{dr_q} \underbrace{g_q(\theta_{dr_q}) \dot{\theta}_{dr_q}}_{-\dot{x}_{dr_q}} \end{aligned} \qquad \{12\}$$

where

$$g_q(\theta_{dr_q}) = \left[r_{dr_q} \sin\theta_{dr_q} + \frac{r_{dr_q}^2 \sin\theta_{dr_q} \cos\theta_{dr_q}}{\sqrt{l_{dr_q}^2 - r_{dr_q}^2 \sin^2\theta_{dr_q}}} \right], \; f_q(\theta_{dr_q}) = g_q(\theta_{dr_q})^2 \qquad \{13\}$$

Note that the equivalent equivalent inertia $J_{eq_{dr_q}}$ and the input disturbance W_{dr_q}

are functions of the crank arm angle. Since rigid elements are assumed to transmit power to the doctor blade assembly, the equivalent inertia and input disturbances are functions of the linear position of the doctor blade. From the dynamics it is evident that the doctor blade motion causes velocity variations at the print cylinder due to variations in equivalent inertia and load disturbance. The variations in both equivalent inertia $J_{eq_{dr_q}}$ and input disturbance W_{dr_q} may be reduced by reducing the stroke length of the doctor blade assembly.

A simple friction model is used to obtain the friction coefficients, F_{pr_q} and F_{dr_q}. The model is a function of the relative velocity between the doctor blade linear velocity and the print cylinder surface velocity. Note that the surface velocity of the print cylinder is much larger in magnitude than the doctor blade velocity. The frictional effect can be resolved into two components to account for friction in the dynamic equations of the print cylinder and the doctor blade assembly. In the friction model both viscous and Coulomb effects are considered, accounting for the lubricating effect of the ink contributing to the viscous friction and the Coulomb frictional effects due to the doctor blade loading. The net friction force is therefore given by

$$F = F_{c_q}\mathrm{sgn}(v_{r_q}) + F_{v_q}v_{r_q}, \qquad v_{r_q} = \sqrt{v_{s_q}^2 + \dot{x}_{dr_q}^2} \qquad \{14a\}$$

$$v_{s_q} = R_{pr_q}\dot{\theta}_{pr_q}, \qquad \dot{x}_{dr_q} = -g_q(\theta_{dr_q})\dot{\theta}_{dr_q} \qquad \{14b\}$$

where F_{c_q}, F_{v_q} are the Coulomb friction coefficient and viscous friction coefficient at print cylinder q, v_{r_q} is the relative velocity between the print cylinder and doctor blade in print unit q, v_{s_q} is the surface velocity of print cylinder q, and r_{pr_q} is the radius of the print cylinder q. Hence the frictional forces in the dynamic equations are given by

$$F_{pr_q} = F\frac{v_{s_q}}{v_{r_q}}, \qquad F_{dr_q} = F\frac{\dot{x}_{dr_q}}{v_{r_q}} \qquad \{15a\}$$

Velocity Dynamics with Web Transport

The print cylinder velocity model presented in the previous section did not include the loading due to the transport of web on it, that is, the print cylinder dynamics without the engagement of the web was presented. Without engaging the print units the web transport is facilitated by the two pull rolls on either side of the print section. When the print units are engaged additional energy from the print cylinders is imparted to the web to further facilitate transport. In this section a model that includes the web dynamics and print cylinder dynamics will be presented.

An impression roller, with a backup roller, is used to nip the web with the print cylinder for efficient transfer of ink from the print cylinder to the web. The nipping action also increases traction between the web and the roller. The following assumptions are considered to obtain a model:

- The coefficient of friction between the web and the impression roll is greater than the coefficient of friction between the web and the print cylinder;
- The web wraps around the impression roller with enough wrap angle, and

adequate nipping force is available to keep the web from slipping on the impression roll. (The web may slip on the print cylinder.)

- The thickness of the web is negligible compared to the radius of the impression roll. Hence it is assumed that the surface velocity of the web is same as the peripheral velocity of the impression roll.
- Since the web is assumed to not slip on the impression roll, the web and the impression roll are considered as one element. The friction forces between the web and the impression roll are ignored and only the friction forces between the web/impression roll and the print cylinder are considered.
- The gravitational effects are ignored and it is assumed that the impression roll loading does not cause any bending.

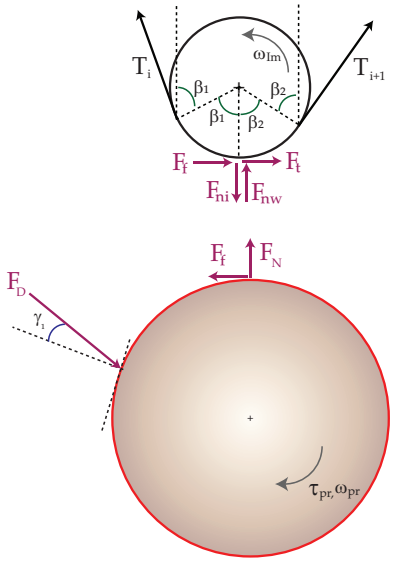

Figure 7: A sketch showing the frictional forces on the print cylinder and the web.

Figure 7 shows the forces involved at the contact of the print cylinder and the impression roll. Let the web wrap around the impression roll with a wrap angle of $\beta_1 + \beta_2$ as shown in the figure, and denote the tension upstream and downstream of the q^{th} print cylinder to be T_{i_q} and T_{i+1_q}. Let F_{D_q} be the force applied on the doctor blade and let γ_{1_q} be the doctor blade contact angle as shown in Figure 7. When the web does not make contact with the print cylinder, the impression roll acts as an idle roller and is driven by the differential tension in the spans upstream and downstream of the roller. When the impression roll is nipped onto the print cylinder, frictional forces between the web and the print cylinder affect the rotational dynamics of the impression roll. In Figure 7, F_t is the force due to the tension differential and F_f is the force due to friction. Based on the wrap angle and the tension upstream and downstream of the impression roll, a normal force F_{nw} acting upwards opposes the nip force F_{ni} and the net normal force is $\mathrm{F}_{\mathrm{N}} = \mathrm{F}_{\mathrm{ni}}$

- F_{nw}. Hence the dynamics for the q^{th} impression roll is given by

$$J_{Im_q}\dot{\omega}_{Im_q} + b_{Im_q}\omega_{Im_q} = r_{Im_q}\left(\mathrm{F}_{t_q} + \mathrm{F}_{f_q}\right) \quad \{16a\}$$

$$\mathrm{F}_{t_q} = T_{i+1_q} - T_{i_q}, \quad \mathrm{F}_{f_q} = f(\mathrm{F}_{\mathrm{N}_q}, \delta_{v_q}) \quad \{16b\}$$

$$\mathrm{F}_{\mathrm{N}_q} = \mathrm{F}_{\mathrm{ni}_q} - \left[T_{i_q}\sin(\beta_1) + T_{i+1_q}\sin(\beta_2)\right], \quad \delta_{v_q} = r_{pr_q}\omega_{pr_q} - r_{Im_q}\omega_{Im_q} \quad \{16c\}$$

The print cylinder dynamics when the impression roll is nipped can be obtained as

$$J_{pr_q}\ddot{\theta}_{pr_q} + b_{pr_q}\dot{\theta}_{pr_q} = K_{gr}\left(\frac{\theta_q}{n_{pr_q}} - \theta_{pr_q}\right) - r_{pr_q}\left(F_{pr_q} + F_{fq}\right) \quad \{17a\}$$

where F_{pr_q} is given by equation $\{15\}$ with $F_{cq} = \mu_{pr_q}\cos(\gamma_{1q})F_{D_q}$; μ_{pr_q} is the friction coefficient between the print cylinder and the doctor blade, γ_{1q} is the doctor blade contact angle, and F_{D_q} is the load force on the doctor blade.

A friction model that includes stiction, Coulomb and viscous effects is considered to describe the friction force between the web and the print cylinder. Since ink fills the grooves in the gravure print cylinder, viscous frictional effects are added to a basic model of friction with Stiction and Coulomb friction effects. Therefore,

$$\mathrm{F}_{f_q} = \begin{cases} \underbrace{\mu_{sw_q}\mathrm{F}_{\mathrm{N}_q}}_{F_{sw_q}}, & \text{if } \delta_{v_q} = 0 \\ \underbrace{\mu_{dw_q}\mathrm{F}_{\mathrm{N}_q}}_{F_{cw_q}}\operatorname{sgn}(\delta_{v_q}) + F_{vw_q}\delta_{v_q}, & \text{otherwise} \end{cases}$$

where μ_{sw_q} is the static friction coefficient, μ_{dw_q} is the dynamic friction coefficient, and F_{vw_q} is the viscous friction coefficient.

The model for registration error given previously did not consider the effect of web slip between the print cylinder and impression roller; the model can be appropriately modified as

$$e_r(t) = l - \int_{t-\tau_1}^{t} \frac{r_{Im_q}\omega_{Im_q}(\tau)}{1+\overline{\epsilon}_{21}(\tau)}d\tau - \left[r_2\theta_2(t) - \frac{r_1\theta_1(t-\tau_1)}{1+\overline{\epsilon}_{21}(t)}\right] + \int_{t-\tau_1}^{t-\tau_2}\dot{\Delta}l(\tau)d\tau. \quad \{18\}$$

The model for the print cylinder velocity dynamics provides a valuable insight into how various mechanical elements can be designed to minimize web strain variations within the print unit. First, the doctor blade assembly must be properly designed with optimal radius and phase for the doctor blade crank arm. The velocity variations in the print cylinders must be minimized; the best design would be to use an independent motor to control the doctor blade motion. Excessive contact force between the doctor blade and print cylinder may result in print cylinder velocity variations and hence a suitable doctor blade loading force need to be maintained. Rate constraints on the compensator motion should also be considered. With appropriate rate constraints, it is possible to minimize the strain variations in the print unit span. Without rate constraints, large strain variations due to compensator motion may result in web slippage on print cylinder, if adequate nipping force is not maintained.

EXPERIMENTS AND MODEL SIMULATIONS

Experimental data from a production press line were collected to corroborate the model developed in the previous sections. Even though web tension was not regulated in the individual print units, load cells were available in the print units to monitor tension. In addition to web tension, registration error data were also available. Measurement of the individual print cylinder velocities were not available. A preliminary analysis of the experimental data to corroborate the model developed is presented in this section; future work will involve model validation with additional measurements by adding sensors to measure print cylinder velocities, etc.

Effect of Doctor Blade Motion

Figure 8 shows tension and registration error data collected during a production run. The top plot shows the tension differential at print cylinder 7 (zero mean); the tension differential is the the difference between the web tension in the upstream and the downstream spans of print cylinder 6. The bottom plot shows the registration error at print unit 7, measured immediately downstream of the print cylinder 7. It is evident that there is a substantial correlation between tension differential and registration error from the plots shown in Figure 8. A frequency domain correlation, using the Fast Fourier Transform (FFT), of the time domain data is shown in Figure 9; the coupling between web tension differential and registration error is evident. Several peaks in the tension data are observed from the FFT plot. All distinct peaks are higher order harmonics of the first peak observed at 0.0315 Hz. Coincidentally, the frequency of oscillation of the doctor blade assembly was also close to this frequency.

Observation of the tension signals upstream and downstream of print cylinder 6 (see Figure 10) indicated that tension disturbances were not transported from upstream and hence they were created in the print unit span possibly[2] due to improper doctor blade configuration.

Comparison of Registration Error from Experiments and Simulations

If the effect of print cylinder velocity variations and compensator motion is ignored in the registration error dynamics described in equation {2}, the model reduces to

$$-\dot{e}_r(t) = \frac{r\omega^*}{1+\overline{\epsilon}_{21}(t)} - \frac{r\omega^*}{1+\overline{\epsilon}_{21}(t-\tau_1)} \qquad \{19\}$$

where ω^* is the angular velocity of the two print cylinders. This model is compared with the following model presented in [4]:

$$\dot{e}_r(t) = \frac{r\omega^*}{1+\epsilon_2(t)} - \frac{r\omega^*}{1+\epsilon_1(t-\tau_1)} \qquad \{20\}$$

In the model presented in this paper, the registration error is a function of differential strain at time t and time $t-\tau_1$ whereas the registration error is a function of upstream strain at time $t-\tau_1$ and downstream strain at time t in [4].

[2]Without measuring individual print cylinder velocities, a direct correlation between doctor blade motion and print cylinder velocity cannot be obtained. Future work will involve collecting additional measurements to complete the model validation

Figures 11 – 14 show comparison of the experimental data and model simulation data from the two models. Data from several production runs were analyzed to obtain the plots. Registration error based on the two models was obtained by using the actual tension data from the press run. A constant web velocity is assumed at all the print cylinders and the effect of compensator motion is neglected (only span length changes are neglected and not the strain dynamics) in the model. In both the figures the top plot compares the actual registration error with output of the model derived in this paper; the bottom plot compares the actual registration error with output of the model presented in [4]. Figure 11 shows the registration error at print unit 7 and Figure 13 shows the registration error at print unit 8. Figure 12 and 14 show a portion of the data from the same production run. From the plots it is evident that the model presented in this paper follows the actual registration error much closer than the model presented in [4]. From these plots it is evident that without considering the effect of print cylinder velocity variations and span length changes due to compensator motion, the model output correlates well with the actual registration error data. It is expected that with additional measurements, such as the print cylinder velocities, compensator rate, one may obtain better correlation between the model output and the measured registration error from experiments.

CONCLUSION AND FUTURE WORK

A model for the registration error in a rotogravure printing press with multiple print units was developed in this paper. Based on the analysis of the model and from experimental data it is evident that the primary cause for misregistration is due to web strain variations. Therefore, to minimize registration error, strain variations must be minimized. In practice, it appears that web tension is seldom regulated within the print units; rather registration error is directly controlled using a compensator roller or by controlling the print cylinder velocities. The work reported in this paper indicates that it will be beneficial to also control tension between two consecutive print cylinders; future work should consider regulation of web tension by possibly using the cooling rollers. Further, future work should also investigate the control algorithms that are used in compensator based printing units such as the one discussed in this paper, and develop algorithms to minimize registration error by considering the strain dynamics within each print unit.

The registration error model presented in this paper was corroborated based on a set of data from actual production runs. The model shows considerable similarity with the actual data collected. Additional measurements are needed to completely validate the model, and to get a better understanding of the causes of registration error; with the current data it is not clear if the compensator motion is the predominant cause for strain variations or the print cylinder velocity variations.

The current trend in printing presses is to use electronic line shafts, instead of mechanical shafts, to synchronize the motion of the print cylinders [5]. By using electronic line shafting, fine control over the print cylinder velocities is achieved and the registration error is controlled without the need for a compensator roll. But from the registration error model developed in this paper it is evident that the strain variations need to be minimized in order to reduce the registration error. It

is hypothesized that a compensator roller in addition to electronic line shafts will provide better registration control compared to the use of just electronic line shafts; future work should involve analysis of the two registration control methods.

It is evident from the dynamic models that registration error dynamics and strain dynamics are not isolated to a single printing unit and in fact registration error in one print unit can result in errors in subsequent print units. Hence it is important to analyze the interaction between different print units based on the model analysis. Development of a suitable control strategy to minimize registration error throughout the print section should also be considered as future work.

ACKNOWLEDGEMENTS

This work was supported by NSF under grant no. 0854612 and OCAST under grant no. AR091-037.

REFERENCES

1. Brandenburg, G., "New Mathematical Models for Web Tension and Register Error," Proceedings of the Third International IFAC Conference on Instrumentation and Automation in the Paper, Rubber and Plastics Industries, 1, pp. 411 – 438, 1976.
2. Branca, C., Pagilla, P. R., and Reid, K. N., "Modeling and identification of the source of oscillations in web tension," Proceedings of the Tenth Intl. Web Handling Conference, 2009.
3. Kolovsky, M. Z., Evgrafov, A. N., Semenov, Yu. A. and Slousch, A. V., " Advanced Theory of Mechanisms and Machines," Foundations of Engineering Mechanics, Springer, 2000.
4. Yoshida, T., Takagi, S., Muto, Y. and Shen, T., "Register Control of Sectional Drive Rotogravure Printing Press," Manufacturing Systems and Technologies for the New Frontier, Springer, 2008, pp. 417 – 420.
5. Brandenburg, G., Geissenberger, S., Kink, C., Schall, N.-H and Schramm, M., "Multimotor electronic line shafts for rotary offset printing presses: a revolution in printing machine techniques," IEEE/ASME Transactions on Mechatronics, vol.4, no.1, pp. 25 – 31, March 1999.

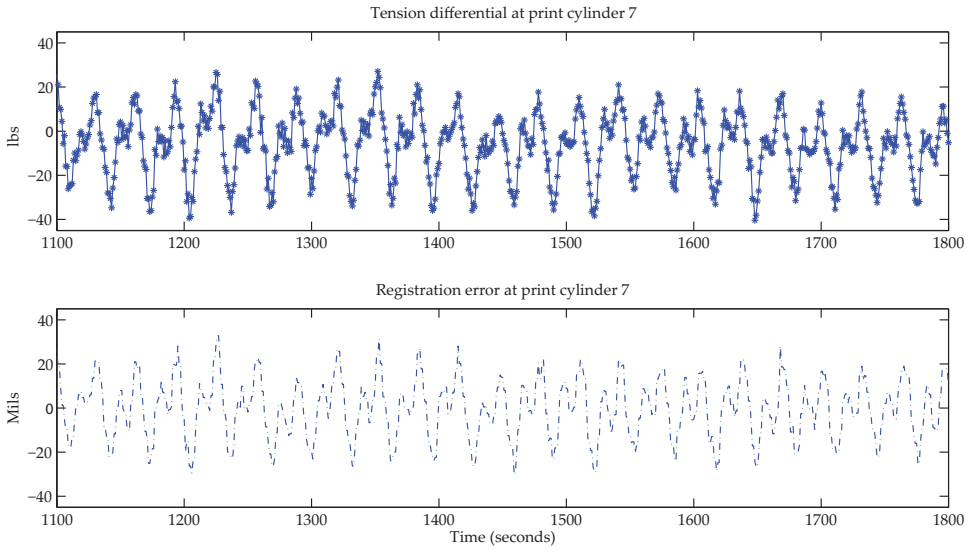

Figure 8: Measured web tension and registration error data in print cylinder 7 from a production run.

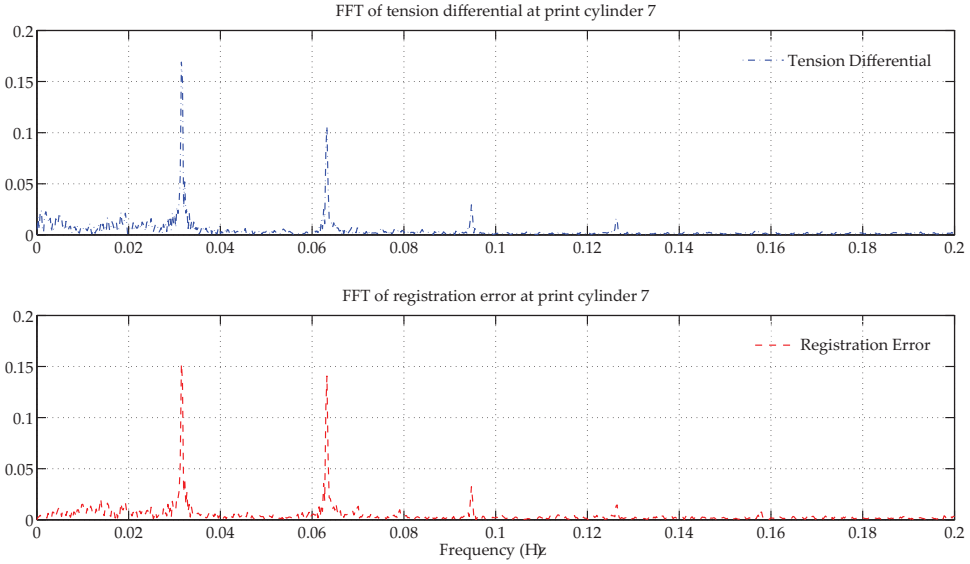

Figure 9: Frequency domain correlation between the tension differential and registration error data in print cylinder 7 from a production run.

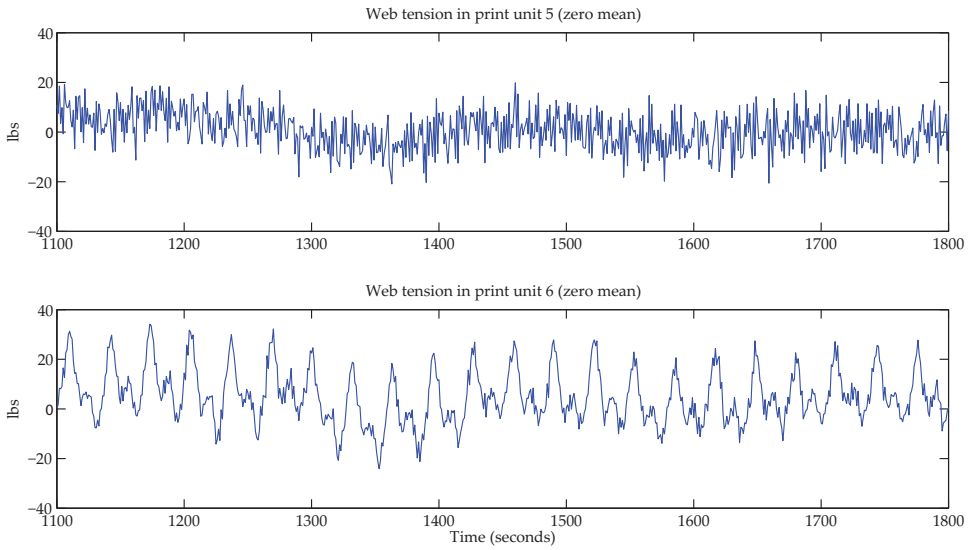

Figure 10: Measured web tension in print unit 5 and print unit 6.

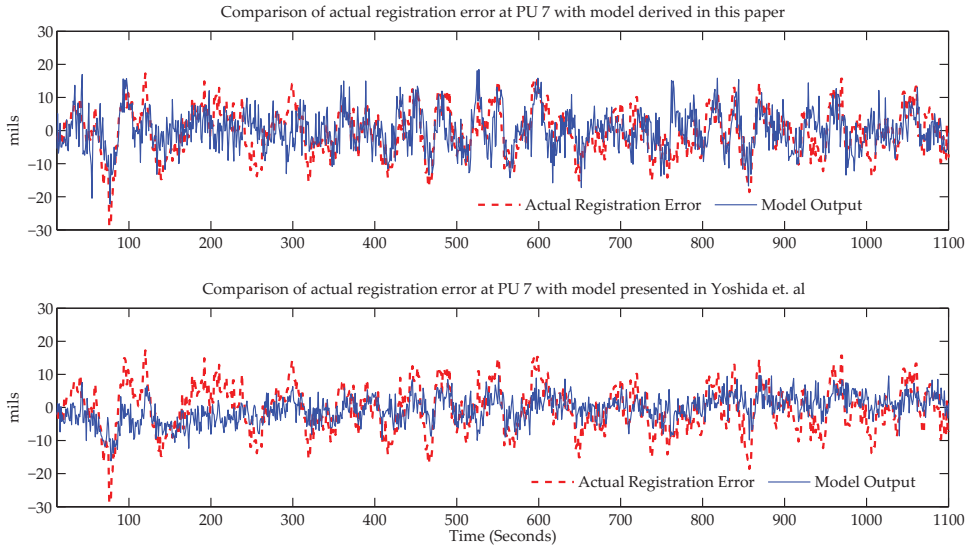

Figure 11: Comparison of model output and measured registration error data for the two models (in print unit 7).

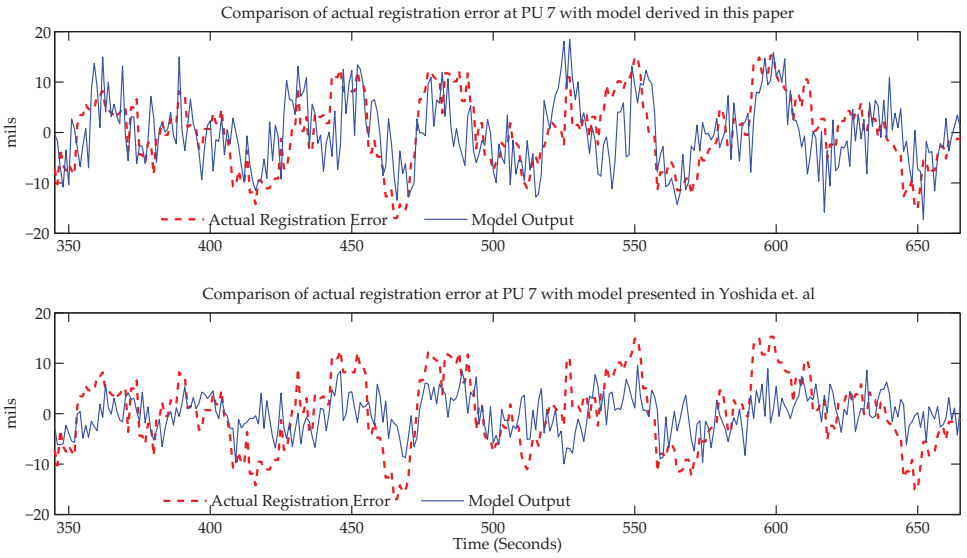

Figure 12: Comparison of model output and measured registration error data for the two models (in print unit 7).

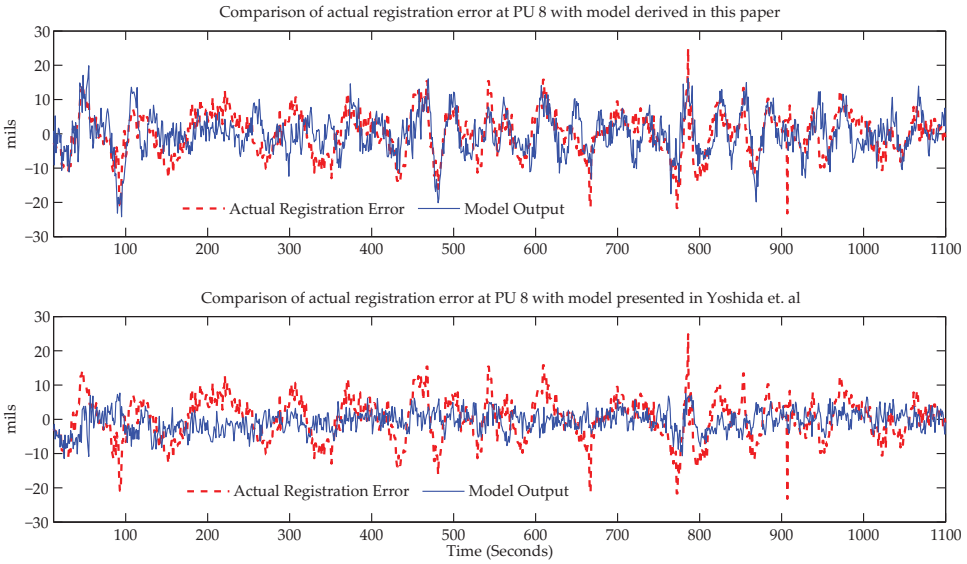

Figure 13: Comparison of model output and measured registration error data for the two models (in print unit 8).

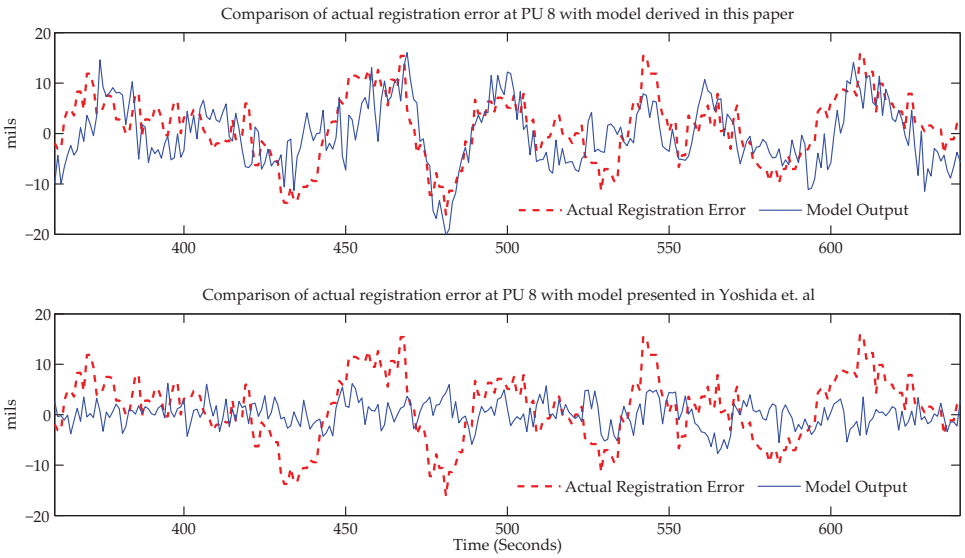

Figure 14: Comparison of model output and measured registration error data for the two models (in print unit 8).